



## In situ measurements of colloid transport and retention using synchrotron X-ray fluorescence

David A. DiCarlo,<sup>1</sup> Yuniati Zevi,<sup>2</sup> Annette Dathe,<sup>2</sup> Shree Giri,<sup>2</sup> Bin Gao,<sup>2</sup> and Tammo S. Steenhuis<sup>2</sup>

Received 13 December 2005; revised 21 July 2006; accepted 18 August 2006; published 17 November 2006.

[1] The physics regarding the retention and mobilization of colloids in saturated and unsaturated conditions remains poorly understood, partially because of the inability to measure colloid concentrations in situ. In this study, we attached Cd<sup>2+</sup> ions to clay colloids and used synchrotron X rays to cause the Cd to fluoresce. By measuring the fluorescence and attenuation of the X rays we obtained simultaneous in situ water saturations and colloid concentrations on timescales of tens of seconds. We used this technique to study the transport of colloids consisting of Na and Ca Montmorillonite clays through a preferential flow path in uniform well-sorted sand. This flow path had both saturated and unsaturated zones that travel downward with time. We found that the Na colloids showed little retention in the sand, while the Ca colloids were retarded with respect to the wetting front. By comparing the results to those obtained by infiltrations with a Cd solute we find that the retention of the colloids seen in the unsaturated portion of the column was no greater than that seen in the saturated portion. We discussed the advantages and limitations of this X-ray fluorescence technique and the implications for colloid transport.

**Citation:** DiCarlo, D. A., Y. Zevi, A. Dathe, S. Giri, B. Gao, and T. S. Steenhuis (2006), In situ measurements of colloid transport and retention using synchrotron X-ray fluorescence, *Water Resour. Res.*, 42, W12S05, doi:10.1029/2005WR004850.

### 1. Introduction

[2] Mobile subsurface colloids play an important role in the translocation of low solubility contaminants [McCarthy and Zachara, 1989; Ryan and Elimelech, 1996; McCarthy and McKay, 2004]. Elevated specific surface areas and charge densities of colloids facilitate the attachment of contaminants [Wan and Tokunaga, 1998], thus potentially mobilizing the contaminants if the colloids themselves are mobile. Movement of colloids in soils has received considerable attention in recent years [Wan and Tokunaga, 1997; Kretzschmar et al., 1999] because the migration of colloids and colloid-contaminant complexes through the soil matrix increases the risk of ground and surface water contamination.

[3] Many studies have been carried out with clay colloids [Compere et al., 2001; Flury et al., 2002; Gao et al., 2004; Zhuang et al., 2003; Chen et al., 2005; Chen and Flury, 2005]. In general retention increases with decreasing moisture content or increasing ionic strength. These findings are derived from column breakthrough experiments rather than in situ measurements of colloid concentrations in the column during the experiment itself.

[4] Micromodels of porous media have been used for visualization of in situ retention and mobilization mechanisms of colloids at the pore scale. The first observations of

retention at the pore-scale were interpreted that colloids are retained at the air/water interface [Wan and Wilson, 1994a; Wan and Tokunaga, 2002]. Recent studies on an open-faced sand pack suggest that the colloids are retained at the air/water/solid contact line [Crist et al., 2004, 2005; Zevi et al., 2005]. Other observations suggest that retention takes place at hydrodynamic dead ends and mobilization is observed to occur on infiltration when the water/air interfaces change position due to increasing water content [Gao et al., 2004].

[5] Concurrently, infiltration events have been shown to mobilize colloids in column and field experiments. Experimental studies use latex microspheres, clays, oxides or microorganisms as the colloids and sand or glass beads as porous media; they may or may not include other tracers. Most infiltration studies performed have been carried out in saturated conditions [Toran and Palumbo 1992; Noell et al., 1998; Jin et al., 2000; Harter et al., 2000; Weisbrod et al., 2003; Chu et al., 2001; Keller et al., 2004]. Fewer have examined infiltration rates less than the saturated condition resulting in unsaturated flow [Wan and Wilson, 1994a, 1994b; Wan and Tokunaga, 1997, 1998, 2001; Schäfer et al., 1998; Thompson et al., 1998; Thompson and Yates, 1999; Jewett et al., 1999; Jin et al., 2000; Gamerding and Kaplan, 2001; Lenhart and Saiers, 2002; Saiers and Lenhart 2003; Gao et al., 2004]. Typically, both types of these experiments involve measuring the colloid concentration in the effluent. Since effluent collection takes place at atmospheric pressure, unsaturated flow experiments usually involve a capillary end effect. In situ measurements of colloid concentration during infiltration events can avoid these end effects by measuring colloid concentrations above the capillary fringe.

<sup>1</sup>National Sedimentation Laboratory, ARS, USDA, Oxford, Mississippi, USA.

<sup>2</sup>Department of Biological and Environmental Engineering, Cornell University, Ithaca, New York, USA.

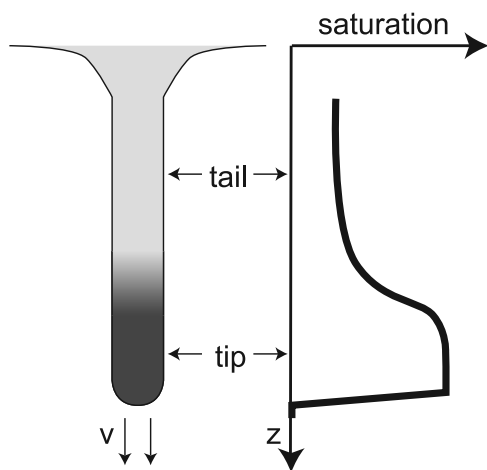


**Figure 1.** Cartoon of a preferential flow path and the associated saturation within the flow path. Preferential flow creates a unique saturation profile with saturated conditions at the tip and unsaturated conditions in the tail. Colloid retention may be affected by the fast moving water/air interfaces.

[6] Synchrotron X rays provide an excellent tool for in situ measurements of colloid concentration due to their penetration through macroscopic slabs of soil. The water saturation within a preferential flow path has been previously measured using a simple absorption technique with monochromatic X rays [Liu *et al.*, 1993; DiCarlo *et al.*, 1997; Bauters *et al.*, 2000]. By adding known concentration of Cd tagged colloids to our infiltrating fluid and measuring the fluorescence of Cadmium at a  $90^\circ$  angle from the X-ray source, we can detect the colloid concentration within the soil rather than just through effluent measurements.

[7] For real 3-D soils, the most likely contributor to colloid transport is through fast preferential flow paths which occur in soils of all types. These paths occur through only a minor portion of the soil, increasing the speed of the infiltrating water front and limiting the filtering ability of the soil. Figure 1 shows a cartoon of a preferential flow path and the saturation within the path. Within a flow path the water saturation shows an abrupt increase followed by a region of large saturation (the finger tip), followed by a decrease in saturation to a constant value (the finger tail). As hydrophobic colloids are expected to cluster at the air/water interfaces, these rapid changes in saturation may or may not retain or mobilize colloids.

[8] In this study, we confine the soil laterally so the preferential flow path is confined. It has been shown that the same saturation behavior is seen in confined preferential flow paths, with the advantage that one knows where the flow path is, and the flux through the flow path [DiCarlo, 2004]. The first objective is to demonstrate the utility of synchrotron X rays for measurements of simultaneous moisture content and colloid concentrations in transient flow. The second objective is to utilize this technique to quantify the transport of Na Montmorillonite clays (Na colloids) and Ca Montmorillonite clays (Ca colloids) within fast preferential flow paths in sandy soils and to assess the

effect of the differential moisture content at the finger tip on the retention and release of these colloids.

## 2. Materials and Methods

### 2.1. Colloids

[9] Cadmium tagged colloids were prepared from  $\text{Na}^+$  and  $\text{Ca}^{2+}$  Montmorillonite clays (SWy-2 and SAz-1 respectively [Costanzo, 2001]) obtained from the Source Clays Repository, Clay Mineral Society, Purdue University. Organic matter was removed by treating 10 g clay with 5 mL 30%  $\text{H}_2\text{O}_2$ . The clay was dispersed in an ultrasonic bath by adding 20 mL of Sodium Hexahydrophosphate and 100 mL distilled water (Na clay pH = 6.2 and Ca clay = 6.5). The mixture was filled to a total of 1000 mL in sedimentation cylinders, and particles  $<1 \mu\text{m}$  diameter were acquired using the sedimentation (pipette) method according to Stokes' law [Dane and Topp, 2000]. As the method is temperature dependent, times for obtaining a clay suspension of 50 mL varied between 13 hours 48 minutes for  $25^\circ\text{C}$  to 12 hours 55 minutes for  $28^\circ\text{C}$ , both at a depth of 5 cm. The procedure was implemented simultaneously in four parallels (called one batch) and repeated several times to get the desired amount of clay. From every batch, an aliquot of 20 mL was dried to estimate the mass of clay in suspension, which was 5.67 mg/mL for Na clay and 1.74 mg/mL for the Ca clay.

[10] To adsorb Cd to the clay, 10 mL of 1000 mg/L Cadmium Nitrate [ $\text{Cd}(\text{NO}_3)_2$ ] was added to 50 mL of clay suspension, shaken for 24 hours, centrifuged and filtered through a  $0.45 \mu\text{m}$  filter. The excess of Cd was removed with 3 washings with deionized distilled water. The concentration of adsorbed Cd was determined as the difference in Cd concentration between the original and the supernatant plus washings solution, measured by an IL-Video12 atomic absorption spectrophotometer (AAS) at 228.8 nm with an air/acetylene flame. The concentrations thus obtained were  $5.94 \mu\text{g}/\text{mg}$  for the Na clay and  $17.3 \mu\text{g}/\text{mg}$  for the Ca clay. A known mass of dry Ca clay with Cd adsorbed was extracted with 50 mL of 0.5M ammonium acetate and shaken for 1 hour. After centrifugation, Cd concentration was measured as  $17.7 \text{ mg Cd/g}$  clay in the aqueous phase.

[11] The concentrations of the Cd clay suspensions as used for the flow experiments with regard to 100 mL distilled water was 2.41 g Na clay to achieve 144 mg/L Cd and 0.58 g Ca clay to achieve 100 mg/L Cd. These are on the high side of typical colloid concentrations as they were chosen to be well above detection limits. In addition to the suspensions, experiments were performed using Cd ( $\text{NO}_3)_2$  solution with 100 mg/L Cd concentration.

### 2.2. Flow Experiment

[12] The flow experiments were conducted in a circular glass column with a length of 40 cm and inner diameter of 1 cm. The column was filled with acid washed dry 30/40 sand (Unimin Corporation, NJ) using a funnel, achieving a porosity of roughly 0.35 and a permeability of 9 cm/min [Schroth *et al.*, 1996]. The working solutions (either Cd-laced colloids or Cd in solution) were infiltrated into the top of the column using a syringe pump at various flow rates less than the saturated conductivity of the sand (9 cm/min). The bottom boundary condition consisted of a screen, with no suction applied, but water freely able to leave. Visually,

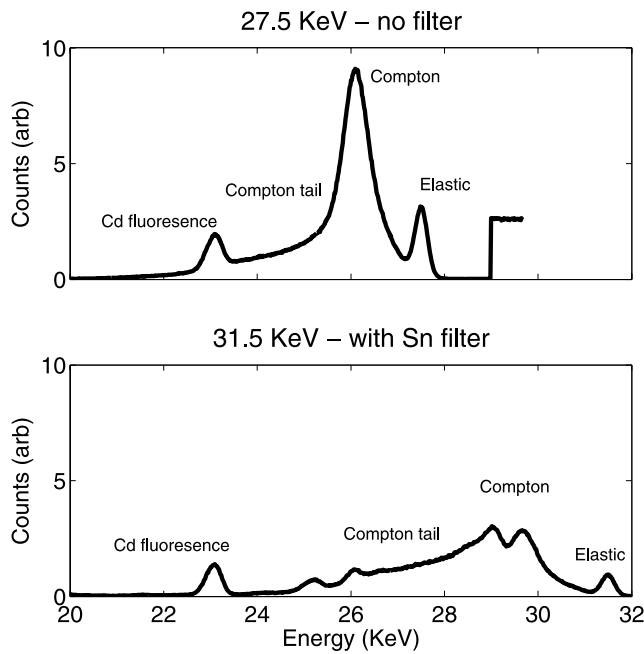


**Figure 2.** X-ray spectrum measured with the Si detector with a sample of 100mg/L Cd in the sample position. The top spectrum is the spectrum obtained with incident X rays of sufficient energy to elicit fluorescence of the Cd, but it has much Compton scattering in the Cd fluorescence window. The bottom spectrum is the one used during the experiment with a higher-energy incident X ray and a Sn filter with much lower background counts.

the water content showed overshoot behavior with a saturated (or nearly saturated) finger tip followed by a decrease in water saturation with time. This produced a mobile water phase with moving water/air interfaces.

[13] Each experiment started with a packed, air-dry column. Three different infiltrating fluxes were used for each of the three different Cd solutions. Water saturations and colloid concentrations were monitored at one point in the column as the wetting front passed through the column. Several infiltrations (hereafter called the flush) with deionized water (pH = 5.6) followed at the same flux as the initial infiltration with the colloid content monitored versus time. For infiltrations of flux 0.26 cm/min, the initial infiltration and flush lasted 30 min, and for infiltrations of flux 1.28 cm/min, the initial infiltration and flush lasted 8 min. After each infiltration or flush the overall column was scanned to measure colloid retention as a function of position within the column.

### 2.3. X-Ray Setup

[14] We performed the X-ray fluorescence experiments at the B-2 beamline at CHESS, an open access synchrotron source in Ithaca, New York. A double bounce Si(220) monochromator converted the white X rays from the bend magnet to monochromatic X rays of energy 31.5 KeV. The X rays passed through a N<sub>2</sub> filled ion chamber at the front of the hutch before striking the experimental column. A N<sub>2</sub> filled ion chamber was placed downstream of the column and a Si solid state detector with energy resolution of

0.05 KeV was placed at 90° angle from the beam direction. The upstream ion chamber was used as a monitor of the incident X rays, and a feedback loop was used to keep the X-ray flux constant throughout a beam fill. The downstream ion chamber was used to measure the transmitted X-ray flux, from which the attenuation and the water content of the column could be calculated.

[15] The solid state detector was used to measure the fluorescence of the Cd in the column which was converted to colloid concentration. Care must be exercised in setting up the fluorescence detector to reduce the background from Compton and elastic scattering from the water and sand in the column. The results of this can be seen in Figure 2 which shows the spectrum of the X rays measured at the Si solid state detector. The top plot is the spectrum using 27.5 KeV with no Sn filter, and the bottom plot is the spectrum using incident X rays of 31.5 KeV with a Sn filter. By choosing a higher incident energy, the Cd fluorescence peak is moved out of the long tail of the Compton scattering from the water phase. The Sn filter consisting of a Sn foil of thickness 58 μm, was placed at the front of the 10 cm flight tube before the Si detector. Sn has an absorption edge at 29.2 KeV, so it preferentially attenuates (by a factor of 4) the Compton scattered X rays above this energy. This dramatically reduced the dead time of the detector, and the overall background.

[16] For calibration and running of the experiments, the output of the Si detector was sent through a pulse shaper and then a single channel analyzer to only count X rays within a range of 0.5 KeV of the Cd fluorescence. Calibration of the detector was done by placing samples of known dissolved Cd, Cd attached to colloids in solution, and a Cd solution in the sand in the column position. Figure 3 shows the measured fluorescent count rate versus Cd concentration for the Na colloids. From these count rates, we estimate that the concentration of Cd can be measured to within 1 mg/L when counting for 5 s with no porous media. Within a porous media (where the porosity is roughly a third), the Cd concentration can be measured to within 2 mg/L for a counting time of 10 s. The calibration was also done with

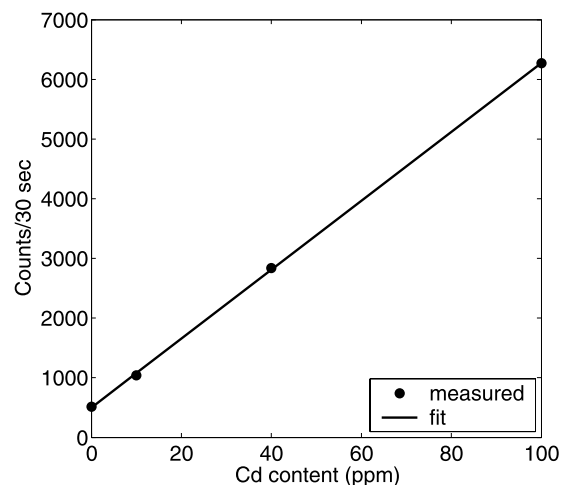


**Figure 3.** Calibration curve for the Na colloids with Cd attached. The Cd content can be determined to an accuracy of 2 mg/L for a 10 s counting time.

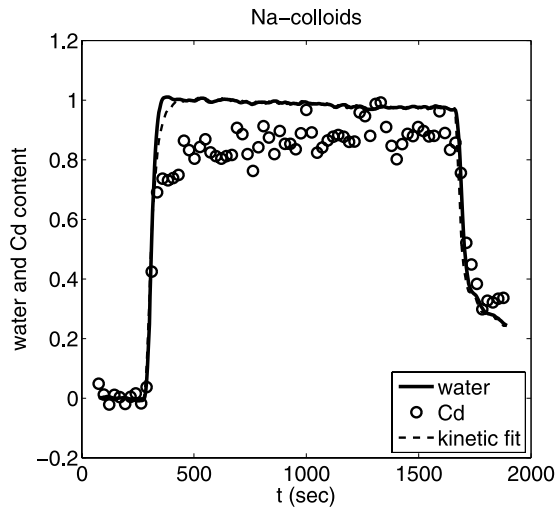


**Figure 4a.** Trace of normalized water and Cd content versus time where the Cd is attached to the Na colloids. The infiltrating flux was 0.26 cm/min, and the observation was made 60 mm below the sand pack surface. The Cd content follows the water content at all times showing that there is no appreciable retention of the Na colloids.

the colloid solutions in porous media (albeit with a smaller array of Cd concentrations) and these calibrations were used for the data obtained during the infiltrations. In terms of colloid concentration, for the colloids used 1 mg/L of Cd corresponds to a colloid concentration of 160 mg/L for the Na colloids and 57 mg/L for the Ca colloids.

[17] In reporting the results, as the Cd ions are attached to the colloids, we use the Cd content as a surrogate for the in situ colloid content during the experiment. The fluorescence technique measures the total mass of Cd that is illuminated by the incoming X-ray beam. This includes Cd that is mobile and Cd that is retained through interactions with the matrix. Mathematically this is represented by

$$Cd_t = Cd_w S_w + Cd_m \quad (1)$$

where  $Cd_t$  is the total Cd content,  $Cd_w$  is the Cd concentration within the water phase, and  $Cd_m$  is the Cd content retained by interactions with the matrix. To normalize the measured fluorescence, the Cd content is normalized such that a value of 1 equals the Cd content that is found for a porous medium saturated with the initial solution ( $Cd_w = 1$ ,  $S_w = 1$ , and  $Cd_m = 0$ ). Note that a single measurement of  $Cd_t$  does not definitively measure the mobile and retained fractions, just the linear combination of the two. Instead the fractions can be obtained by using the time evolution of the total Cd content and a simple advection-dispersion model as explained below.

#### 2.4. Kinetic Model

[18] The one dimensional advection-dispersion equation was used to describe the transport of Cd in the column,

$$\frac{\partial}{\partial t} Cd_w + \frac{\partial}{\partial t} Cd_m = D \frac{\partial^2}{\partial z^2} Cd_w - v \frac{\partial}{\partial z} Cd_w \quad (2)$$

where  $D$  is the dispersion,  $v$  is the velocity of the front, and the initial condition is  $Cd_w = Cd_m = 0$  for  $z > 0$ ,  $t = 0$  and the boundary condition is  $Cd_w = 1$  for  $z = 0$ ,  $t > 0$ . The matrix concentration  $Cd_w$  can be described by first order kinetics:

$$\frac{\partial}{\partial t} Cd_m = K_a Cd_w - K_d Cd_m \quad (3)$$

where  $K_a$  is the attachment rate of the colloids to the matrix, and  $K_d$  is the detachment rate.

[19] To fit this to the data, we numerically solved the coupled equations with the velocity obtained from measurements of the wetting front versus time. The dispersion ( $D = 0.004 \text{ cm}^2/\text{s}$ ) was fixed for all infiltrations, and  $K_a$  and  $K_d$  were fit for each colloid/solute. These fits are shown as a dashed line in the subsequent plots of Cd content versus time. Importantly, this model assumes that there is no extra retention when the media becomes unsaturated, and thus will only provide a good fit to the data if this is the case.

### 3. Results

#### 3.1. Initial Infiltration

[20] Figure 4a shows the normalized water and Cd content versus time for the Na colloid solution. The measurement point was 60 mm below the sand surface, and the infiltrating flux was 0.26 cm/min. The water content is in units of saturation (volumetric water/porosity) where a value of 1 is completely saturated. The water content starts at zero then jumps to fully saturated at the arrival of the wetting front. This is followed by a decrease in saturation as the wetting front moves downward. This behavior versus time matches the typical saturation overshoot pattern measured previously in slab and column experiments of similar sand [Bauters *et al.*, 2000].

[21] Figure 4a shows that the total Cd content closely follows the water saturation with a large initial jump followed by a decrease in Cd as the wetting front moves downward, with this decrease proportional to the decrease

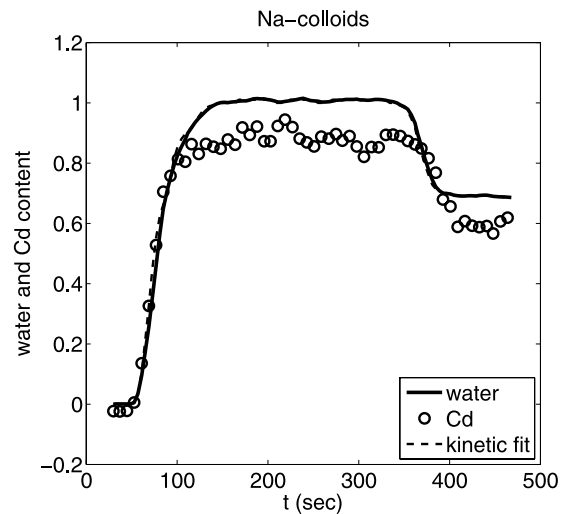


**Figure 4b.** Trace of normalized water and Cd content versus time where the Cd is attached to Na colloids. At a higher flux of 1.28 cm/min, the behavior is very similar to that seen at the lower flux (Figure 4a).

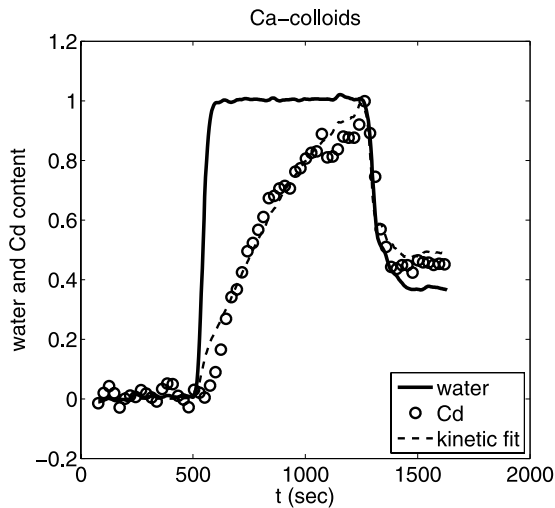


**Figure 5a.** Trace of normalized water and Cd content versus time where the Cd is attached to the Ca colloids. The infiltrating flux was 0.26 cm/min, and the observation was made 60 mm below the sand pack surface. The water content shows similar behavior to the infiltration using the Na colloids, but the Cd content (attached to the Ca colloids) shows a delayed response with respect to the water.

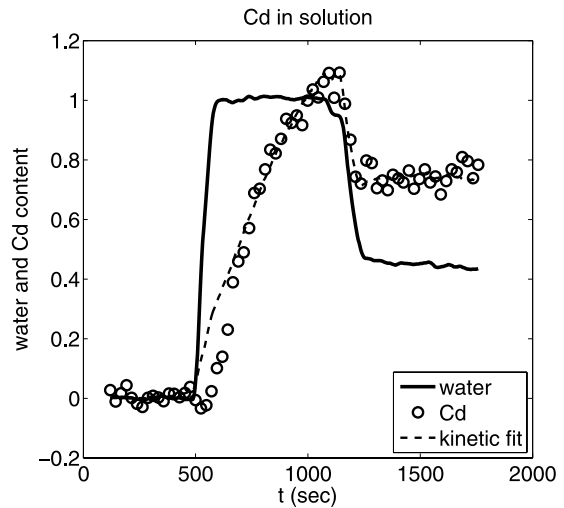


**Figure 6a.** Trace of normalized water and Cd content versus time where the Cd is in solution. The infiltrating flux was 0.26 cm/min, and the observation was made 60 mm below the sand pack surface. Again the water content behavior is similar to the other infiltrations. For the Cd in solution a delayed response with respect to the water is observed, similar to that seen for the Cd attached to the Ca colloids.

in water content. Since the Cd content closely tracks the water saturation, this implies that the Cd (and the Na colloids to which it is attached) remains suspended in solution, and that no significant attachment of the Cd is observed for the initial infiltration. This is shown as the model gives a reasonable fit with  $K_a = K_d = 0$ , implying no attachment of the Na colloids. Surprisingly, the Cd level observed in the finger tip never quite reaches the saturated value, as predicted from the model.

[22] Figure 4b shows the same Na colloids but an infiltration with a higher flux (1.28 cm/min). No retention or retardation is seen, and the fit with  $K_a = K_d = 0$  is reasonable.

[23] Figure 5a shows the infiltration for the Ca colloids at the same point and same infiltration rate as Figure 4a. The water saturation shows similar changes with time as for the Na colloid experiment, but the Cd content exhibits a different behavior. Here the Cd content rises well after the initial water saturation. It eventually reaches a level greater

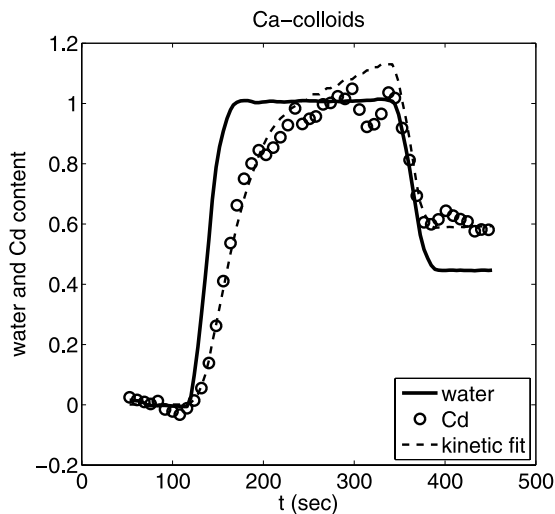


**Figure 5b.** Trace of normalized water and Cd content versus time where the Cd is attached to Ca colloids. At a higher flux of 1.28 cm/min the behavior is very similar to that seen at the lower flux (Figure 5a).

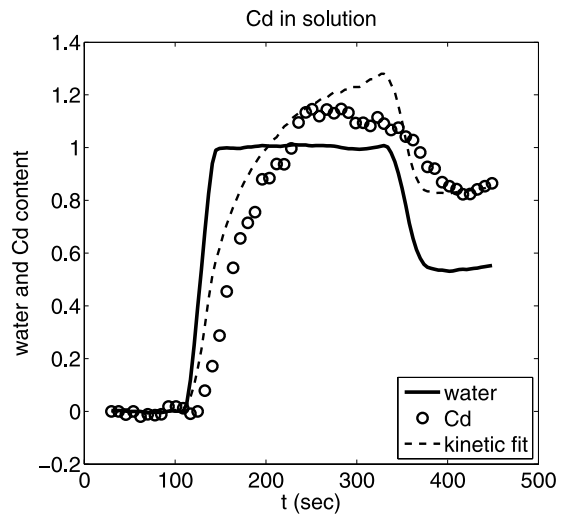


**Figure 6b.** Trace of normalized water and Cd content versus time where the Cd is in solution for a higher flux of 1.28 cm/min. The behavior is very similar to that seen at the lower flux (Figure 6a).

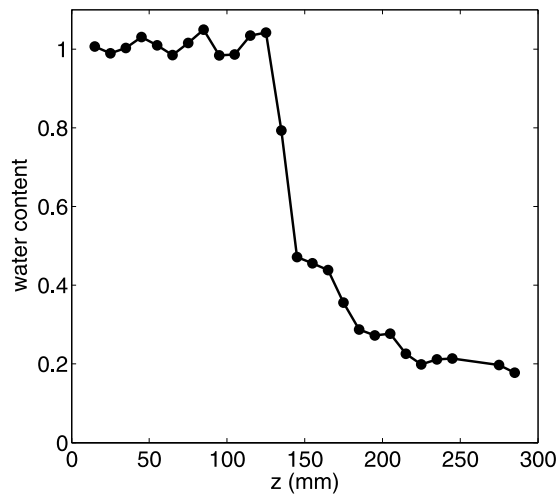


**Figure 7.** Water content versus height in the column after infiltrations (with colloids or without). Water is retained at the bottom of the column because of capillary forces, and the curve resembles the soil characteristic curve.

than the Cd content of the initial fluid. After the water saturation drops behind the saturated tip, the Cd concentration also drops, but remains above the level of Cd in the initial fluid. Thus some Cd (and Ca colloids) are being retained on the drying cycle.

[24] The kinetic model produces a qualitative fit with  $K_a = 0.0058 \text{ s}^{-1}$ ,  $K_d = 0.019 \text{ s}^{-1}$ . The attachment in the model causes the initial Cd front to be retarded with respect to the water front. It also predicts that the Cd content becomes greater than the water saturation, which is what is expected when the colloids are retained. This is true in the saturated finger tip and unsaturated finger tail. Figure 5b is for the higher flux, showing similar behavior with a reasonable fit  $K_a = 0.0072 \text{ s}^{-1}$ ,  $K_d = 0.024 \text{ s}^{-1}$ .

[25] Figure 6a shows the infiltration at the same rate for the Cd in solution instead of attached to the colloids. Here we see the behavior is similar to the Ca colloids with a delayed response of the Cd, and retention of the Cd behind on the drying cycle. Again, the kinetic model fit works well, this time with  $K_a = 0.0020 \text{ s}^{-1}$ ,  $K_d = 0.013 \text{ s}^{-1}$ . Figure 6b is for the higher flux, showing similar behavior with a reasonable fit  $K_a = 0.0026 \text{ s}^{-1}$ ,  $K_d = 0.017 \text{ s}^{-1}$ .

[26] In addition, to the measurements of the water saturation and colloid content at a single point, during the initial infiltration the entire column was scanned vertically at 10 cm intervals. Figure 7 shows the water content versus space after the initial infiltration. The water content shows a typical water saturation versus height for the sandy medium with a saturated portion in the bottom half of the column, corresponding to the capillary fringe, and a quick transition to lower water contents above the fringe. As expected, this pattern of water content versus height did not depend on the colloid solution used.

[27] Figure 8 shows the Cd content versus height during the 0.26 cm/min infiltrations when the wetting front had reached the bottom of the column. At heights below the water fringe ( $z < 150 \text{ mm}$ ), the Cd content is close to the Cd content within the initial fluid for all of the solutions. At heights above the water fringe ( $z > 150 \text{ mm}$ ), the most

retention of Cd is observed for the Cd in solution, followed by the Cd attached to Ca colloids, and finally by the Cd attached to the Na colloids. This matches the retention observed versus time at a point in the top half of the column (Figures 4a–6b).

### 3.2 Water Flushing

[28] After the initial infiltration with the colloidal solution, we performed two subsequent infiltrations with distilled, deionized (DDI) water to observe the retention of colloids in the column. After each infiltration, the column was scanned vertically to measure the water and Cd concentration versus position along the column.

[29] Figure 9 shows the Cd content versus height after the 0.26 cm/min infiltrations and flushes for all three initial colloid solutions. Again, the greatest Cd retention is seen for the Cd solution and the Ca colloids, with the lowest amount seen for the Na colloids. For each solution, the Cd contents are roughly constant with height even though the bottom of the column ( $z < 150 \text{ mm}$ ) was below the capillary fringe and thus saturated, while the top of the column ( $z > 150 \text{ mm}$ ) was unsaturated with a low water saturation ( $S_w = 0.2$ ). This further suggests that there was no observed extra retention of the colloids or solutes in the unsaturated zone compared to the saturated zone.

[30] One experiment was performed at a low infiltrating flux rate of 0.064 cm/min. This allowed the column to be scanned vertically throughout the subsequent flush with DDI water, obtaining Na colloid contents versus vertical distance and time (in the other experiments the passage of the front was too fast to be monitored in this fashion). Figure 10 depicts the dynamics of the Na colloids during the pure water flush. As can be seen, the Na colloids form a bank at the front of the invading water flush. The Na colloid

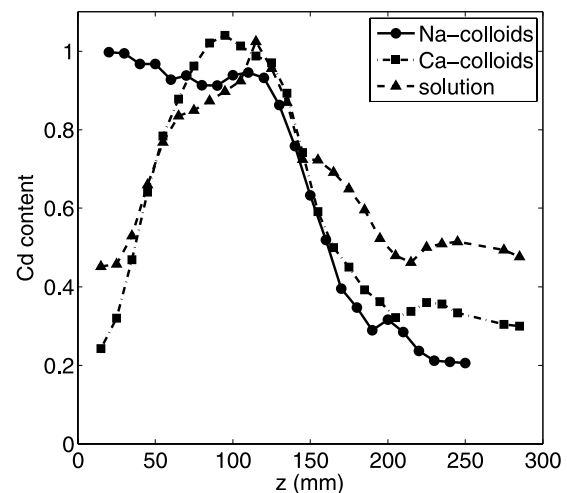


**Figure 8.** Cd content versus height during the initial infiltration for Cd attached to Na and Ca colloids and for Cd in solution. The Cd in solution is retained the most, while the Cd content for the Na colloids basically matches the water saturation (in other words, all the Na colloids are still in solution). The Cd content for the Ca colloids is basically between the two. Note that the drop-off in content near  $z = 0$  for the Ca and Cd in solution is due to the Cd front being retarded with respect to the saturation front.

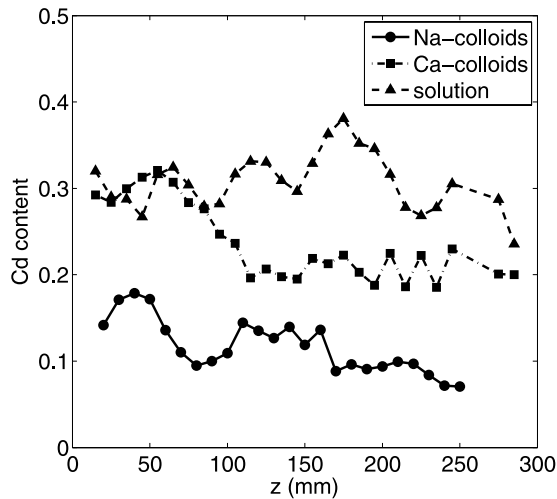


**Figure 9.** Cd content versus height after two flushes of two pore volumes of DI water for Cd attached to Na and Ca colloids and for Cd in solution. Again the Cd content observed is greatest for the Cd in solution and least for the Cd attached to the Na colloids. After the two flushes, the retention of the colloids is relatively constant versus height, with no significant difference between the saturated zone ( $z < 150$  mm) and the unsaturated zone ( $z > 150$  mm).

content reaches levels over 60% greater than in the initial solution. Thus there is mobilization of previously retained colloids during this flush. In contrast, the water saturation changed less than 1% during the flush (not shown). The small change in saturation is entirely due to the low infiltration flux, a much higher flux would have necessarily altered the saturation.

#### 4. Discussion

[31] It is apparent from these in situ measurements that the Na colloids remain suspended during infiltration, whether in the saturated front of the infiltration or the unsaturated region behind the initially saturated front. There was no retardation of the Na colloids in the initial front, as it arrived at the same time as the water front. The Na colloid saturation in the unsaturated region behind the front followed the water saturation (thus the Na colloid concentration was uniform throughout) for all of the experiments. No excess retention is found with the creation of air/water interfaces behind the saturated front.

[32] In contrast, the Ca colloids show a retardation with the infiltrating front, and an excess behind the front. After the initial front hit the observation point, it takes an extra 150 sec for the colloid concentration to reach half its saturated value. The observed retardation and retention matches well a simple kinetic model for the colloids retention. It appears that this retention is just due to the interaction with the solid surfaces, and not with the air-water interfaces as no excess retention is seen in the unsaturated portion, and the model matches the results well in both the saturated tip and the unsaturated tail. Thus although there is an excess of colloids in the unsaturated portion of the infiltration (the colloid saturation is higher

than the water saturation), this is the same excess seen in the saturated portion of the infiltration.

[33] This interpretation is strengthened by the observations of the Cd in solution infiltration. These infiltrations (Figures 6a and 6b), are very similar to those with Ca colloids with a slightly larger retention isotherm. The fit to the kinetic model is just as good as the Ca colloid fit. However, as the Cd in solution has a negligible affinity to the air/water interfaces, it is reasonable to assume that the observed retention is only due to ion sorption to the solid surfaces, and not due to any interactions with the air/water interfaces. This furthers the interpretation that even for this mildly sorbing Ca colloid, there is no extra retention with the creation of air/water interfaces behind the saturated front.

[34] As mentioned earlier, currently one of the limitations of the technique was the use of a very high concentration of colloids (1.6% for the Na colloids, and 0.57% for the Ca colloids). From the detection limits of our experiment, we could only resolve excess retention if it was approximately 10 mg/L of Cd in the unsaturated zone. This corresponds to a colloid concentration of 570 mg/L by weight for the Ca colloids. This seems like a large amount of colloids to be retained at the air-water interfaces.

[35] On subsequent flushes with DDI water we observe that Cd still exists in the column, even for Na colloids that appear to have no affinity to the solid surfaces. One possible explanation is that in this case before the flush, the water within the column still has the Na colloids suspended. However, the water phase may become poorly connected due to the low saturations that are achieved. On subsequent flushes with DDI water, water pockets may not come in contact with the flushing water, leaving behind the suspended colloids. Although within the saturated zone, this does not seem likely to be the case, as the water is well connected, and there still is some retention of Na colloids in

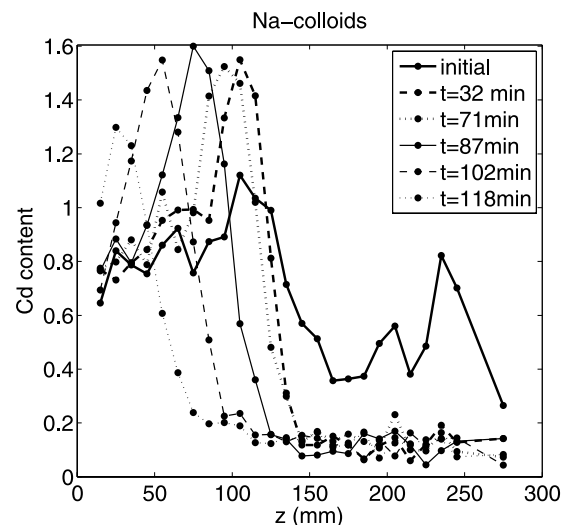


**Figure 10.** Na colloid content versus space and time for a slow flush with DI water. The colloid content forms a bank at the leading edge of the displacing water. This bank has colloid content over 60% higher than the initial infiltrating mixture.

this zone. In either case, the excess is greater for the solutions that are retained on the initial infiltration. This suggests that there is some latency with the retention in the sense that the colloids do not immediately remobilize when the solution has a lower colloid concentration than the matrix.

[36] Possibly the most interesting preliminary result from this study is the dynamics of mobilization seen in the slow flush for the Na colloids in Figure 10. On the slow flush with colloid free water, the bank of colloids that is produced in some cases reaches a level 60% greater than the concentration in the original influent. It is interesting that this mobilization occurs with only a negligible change in water content in this unsaturated zone. This is in contrast with some predictions that mobilization depends on the specific water content [Gao et al., 2004], and thus may be a fruitful avenue for future research.

## 5. Conclusion

[37] In summary, we show that a combination of X-ray fluorescence and transmission can provide accurate and quick in situ measurements of colloid concentration and water saturation. We observe that the Na colloids show no appreciable retention with the porous medium, while the Ca colloids show attachment with the solid phase in the column consistent with a simple kinetic model. Somewhat surprisingly, we observe no measurable excess retention of colloids when the flow switches from saturated (at the finger tip) to unsaturated (the finger tail). Finally, we observe mobilization of a bank of colloids when water is flushed through the column where colloids have been previously retained.

[38] **Acknowledgments.** This work is based upon research conducted at the Cornell High Energy Synchrotron Source (CHESS) which is supported by the National Science Foundation under award DMR-0225180. The authors thank Robert Wells and the three anonymous reviewers for their insightful comments, which greatly improved the manuscript.

## References

- Bauters, T. W. J., D. A. DiCarlo, T. S. Steenhuis, and J.-Y. Parlange (2000), Soil water content dependent wetting front characteristics in sands, *J. Hydrol.*, 231–232, 244–254.
- Chen, G., and M. Flury (2005), Retention of mineral colloids in unsaturated porous media as related to their surface properties, *Colloids Surf. A*, 256, 207–216.
- Chen, G., M. Flury, J. B. Harsh, and P. C. Lichtner (2005), Colloid-facilitated transport of cesium in variably-saturated Hanford sediments, *Environ. Sci. Technol.*, 39, 3435–3442.
- Chu, Y., Y. Jin, M. Flury, Y. Zevi, P. C. Yavey, J. A. Throop, and T. S. Steenhuis (2001), Mechanisms of virus removal during transport in unsaturated porous media, *Water Resour. Res.*, 37, 253–263.
- Compere, F., G. Porel, and F. Delay (2001), Transport and retention of clay particles in saturated porous media: Influence of ionic strength and pore velocity, *J. Contam. Hydrol.*, 49, 1–21.
- Costanzo, P. M. (2001), Baseline studies of the clay minerals society source clays: Introduction, *Clays Clay Miner.*, 49(5), 372–373.
- Crist, J. T., J. F. McCarthy, Y. Zevi, P. C. Yavey, J. A. Throop, and T. S. Steenhuis (2004), Pore-scale visualization of colloid transport and retention in partly saturated porous media, *Vadose Zone J.*, 3(2), 444–450.
- Crist, J. T., Y. Zevi, J. F. McCarthy, J. Troop, and T. S. Steenhuis (2005), Transport and retention mechanisms of colloids in partially saturated porous media, *Vadose Zone J.*, 4, 184–195.
- Dane, J. H., and G. C. Topp (Eds.) (2000), *Methods of Soil Analysis*, part 4, *Physical Methods*, p. 272, Soil Sci. Soc. of Am., Madison, Wis.
- DiCarlo, D. A. (2004), Experimental measurements of saturation overshoot on infiltration, *Water Resour. Res.*, 40, W04215, doi:10.1029/2003WR002670.
- DiCarlo, D. A., T. W. J. Bauters, T. S. Steenhuis, J.-Y. Parlange, and B. R. Bierck (1997), High-speed measurements of three-phase flow using synchrotron X rays, *Water Resour. Res.*, 33, 569–576.
- Flury, M., J. B. Mathison, and J. B. Harsh (2002), In situ mobilization of colloids and transport of cesium in Hanford sediments, *Environ. Sci. Technol.*, 36, 5335–5341.
- Gamerding, A. P., and D. I. Kaplan (2001), Physical and chemical determinants of colloid transport and deposition in water-unsaturated sand and Yucca mountain tuff material, *Environ. Sci. Technol.*, 35, 2497–2504.
- Gao, B., J. E. Saiers, and J. N. Ryan (2004), Deposition and mobilization of clay colloids in unsaturated porous media, *Water Resour. Res.*, 40, W08602, doi:10.1029/2004WR003189.
- Harter, T., S. Wagner, and E. R. Atwill (2000), Colloid transport and filtration of *Cryptosporidium parvum* in sandy soil and aquifer sediments, *Environ. Sci. Technol.*, 34, 62–70.
- Jewett, D. G., B. E. Logan, R. G. Arnold, and R. C. Bales (1999), Transport of *Pseudomonas fluorescens* strain P17 through quartz sand columns as a function of water content, *J. Contam. Hydrol.*, 36, 73–89.
- Jin, Y., Y. J. Chu, and Y. S. Li (2000), Virus removal and transport in saturated and unsaturated sand columns, *J. Contam. Hydrol.*, 43, 111–128.
- Keller, A. A., S. Sirivithayapakorn, and C. V. Chrysikopoulos (2004), Early breakthrough of colloids and bacteriophage MS2 in a water-saturated sand column, *Water Resour. Res.*, 40, W08304, doi:10.1029/2003WR002676.
- Kretzschmar, R., M. Borkovec, D. Grolimund, and M. Elimelech (1999), Mobile surface colloids and their role in contaminant transport, *Adv. Agronom.*, 66, 121–193.
- Lenhart, J. J., and J. E. Saiers (2002), Transport of silica colloids through unsaturated porous media: Experimental results and model comparisons, *Environ. Sci. Technol.*, 36, 769–777.
- Liu, Y., B. R. Bierck, J. S. Selker, T. S. Steenhuis, and J.-Y. Parlange (1993), High intensity X-ray and tensiometer measurements in rapidly changing preferential flow fields, *Soil Sci. Soc. Am. J.*, 57, 1188–1192.
- McCarthy, J., and L. McKay (2004), Colloid transport in the subsurface, *Vadose Zone J.*, 3, 326–337.
- McCarthy, J. F., and J. M. Zachara (1989), Subsurface transport of contaminants-mobile colloids in the subsurface environment may alter the transport of contaminants, *Environ. Sci. Technol.*, 23, 496–502.
- Noell, A. L., J. L. Thompson, M. Y. Corapcioglu, and I. R. Triay (1998), The role of silica colloids on facilitated cesium transport through glass bead columns and modeling, *J. Contam. Hydrol.*, 31, 23–56.
- Ryan, J. N., and M. Elimelech (1996), Colloid mobilization and transport in groundwater, *Colloids Surf. A*, 107, 1–56.
- Saiers, J. E., and J. J. Lenhart (2003), Colloid mobilization and transport within unsaturated porous media under transient-flow conditions, *Water Resour. Res.*, 39(1), 1019, doi:10.1029/2002WR001370.
- Schäfer, A., P. Ustohal, H. Harms, F. Stauffer, T. Dracos, and A. J. B. Zehnder (1998), Transport of bacteria in unsaturated porous media, *J. Contam. Hydrol.*, 33, 149–169.
- Schroth, M. H., S. J. Ahearn, J. S. Selker, and J. D. Istok (1996), Characterization of Miller-similar silica sands for laboratory hydrologic studies, *Soil Sci. Soc. Am. J.*, 60, 1331–1339.
- Thompson, S. S., and M. V. Yates (1999), Bacteriophage inactivation at the air-water-solid interface in dynamic batch systems, *Appl. Environ. Microbiol.*, 65, 1186–1190.
- Thompson, S. S., M. Flury, M. V. Yates, and W. A. Jury (1998), Role of the air-water-solid interface in bacteriophage sorption experiments, *Appl. Environ. Microbiol.*, 64, 304–309.
- Toran, L., and A. V. Palumbo (1992), Colloid transport through fractured and unfractured laboratory sand columns, *J. Contam. Hydrol.*, 9(3), 289–903.
- Wan, J., and T. K. Tokunaga (1997), Film straining of colloids in unsaturated porous media: Conceptual model and experimental testing, *Environ. Sci. Technol.*, 31(8), 2413–2420.
- Wan, J., and T. K. Tokunaga (1998), Measuring partition coefficients of colloids at air-water interfaces, *Environ. Sci. Technol.*, 32, 3293–3298.
- Wan, J., and T. K. Tokunaga (2001), Surface-zone flow along unsaturated rock fractures, *Water Resour. Res.*, 37(2), 287–296.
- Wan, J., and T. K. Tokunaga (2002), Partitioning of clay colloids at air-water interfaces, *J. Colloid Interface Sci.*, 247, 54–61.

- Wan, J., and J. L. Wilson (1994a), Visualization of the role of the gas-water interface on the fate and transport of colloids in porous media, *Water Resour. Res.*, *30*(1), 11–23.
- Wan, J., and J. L. Wilson (1994b), Colloid transport in unsaturated porous media, *Water Resour. Res.*, *30*(4), 857–864.
- Weisbrod, N., M. R. Niemet, and J. S. Selker (2003), Light transmission technique for the evaluation of colloidal transport and dynamics in porous media, *Environ. Sci. Technol.*, *37*, 3694–3700.
- Zevi, Y., A. Dathe, J. F. McCarthy, B. K. Richards, and T. S. Steenhuis (2005), Distribution of colloid particles onto interfaces in partially saturated sand, *Environ. Sci. Technol.*, *39*, 7055–7064.
- Zhuang, J., M. Flury, and Y. Jin (2003), Colloid-facilitated Cs transport through water-saturated Hanford sediment and Ottawa sand, *Environ. Sci. Technol.*, *37*, 4905–4911.

---

D. A. DiCarlo, National Sedimentation Laboratory, ARS, USDA, PO Box 1157, Oxford, MS 38655, USA. (ddicarlo@ars.usda.gov)

A. Dathe, B. Gao, S. Giri, T. S. Steenhuis, and Y. Zevi, Department of Biological and Environmental Engineering, Cornell University, Ithaca, NY 14853, USA.